Susceptibility scaling and vertex corrections for a nested Fermi liquid

A. Virosztek
Institute of Physics, Technical University of Budapest, H-1525 Budapest, Hungary
and Research Institute for Solid State Physics and Optics, POB. 49, H-1525 Budapest, Hungary

J. Ruvalds
Physics Department, University of Virginia, Charlottesville, Virginia 22903
(Received 13 July 1998)

An unusual scaling of the spin susceptibility, as a function of frequency/temperature, was discovered for noninteracting electrons on a nested Fermi surface. This scaling has been confirmed by neutron-scattering experiments on high-temperature superconductors, and it can explain the anomalous quasiparticle damping in cuprates if electron collisions are dominant. The present work proves that self-energy and vertex corrections preserve the scaling features of the susceptibility to leading order in the Hubbard on-site Coulomb repulsion U. Analytic results for the static susceptibility show how self-energy and vertex terms modify the traditional random-phase approximation results for a spin-density-wave instability and suppress the charge susceptibility. These results are relevant to d-wave superconductors, organic metals, and chromium.
[S0163-1829(99)02402-9]

I. INTRODUCTION

The Landau Fermi-liquid theory of weakly interacting quasiparticles is valid in simple metals because the Pauli exclusion principle limits accessible scattering states.[1] Luttinger proved[2] that the damping for electron collisions on a Fermi sphere takes the Fermi-liquid (FL) form

$$\Gamma_{FL}=A[(\pi T)^2+\omega^2], \tag{1}$$

where the small prefactor A is determined by the Coulomb potential. Higher-order self-energy and vertex corrections renormalize the constant A, but otherwise yield corrections of higher powers in the frequency ω and temperature T. This perturbation theory justifies the free-electron response of electrons in a simple metal, which Drude deduced a hundred years ago from the optical conductivity spectra of metals like copper, silver, and even lead.

However, many metals exhibit anomalous damping that is dominated by electron collisions. For example, high-temperature superconductors, such as the cuprate $YBa_2Cu_3O_7$, display a damping that is linear in ω up to large frequencies $\approx$1 eV and that becomes linear in T in the static limit.[3] If the linear damping persists to zero frequency, causality forces the effective mass to diverge at zero temperature and frequency—a scenario that is the essence of the ''marginal'' Fermi-liquid hypothesis.[4]

The present analysis is motivated by the nested Fermi-liquid theory[5] (NFL) that derives the unconventional damping

$$\Gamma_{NFL}\simeq\frac{\pi}{2}[U/W]^2\ \max|\omega,(\pi-2)T| \tag{2}$$

by applying the Born approximation to electrons scattering between nearly parallel segments of the Fermi surface, which are separated by a momentum $\mathbf{Q}$. When the quasiparticle energy spectrum satisfies the nesting condition

$$\varepsilon_0(\mathbf{k}+\mathbf{Q})\simeq-\varepsilon_0(\mathbf{k}), \tag{3}$$

the phase space for collisions is dominated by parallel orbit regions.

When the NFL damping formula is fit to experimental transport data on cuprates, the estimated Hubbard on-site Coulomb repulsion U is similar to the bandwidth W. Thus higher-order corrections are needed to test the self-consistency of the NFL theory.

The primary goal of the present analysis is to compute the self-energy and vertex corrections to the spin susceptibility, since the susceptibility scaling as a function of (ω/T) determines the anomalous NFL damping. We find a strong renormalization of the susceptibility by the self-energy and the vertex terms, and prove that the scaling is conserved in leading orders of U.

Vertex corrections cancel divergent self-energy contributions to the optical conductivity in the long-wavelength limit, as shown by a charge-conserving analysis that satisfies the Ward identity.[6] These NFL calculations provide a microscopic explanation for two mysterious features of superconducting cuprates: The strange decrease in the optical reflectivity as a function of ω;[6] and a flat electronic Raman spectrum that persists to 1 eV.[7]

The susceptibility at finite momentum plays a key role in d-wave superconductivity theories and defines a phase diagram for the competing spin-density-wave (SDW) phase transition.[8] Decades ago, Berk and Schrieffer,[9] and independently Kohn and Luttinger,[10] showed that pairing by exchange of spin or charge fluctuations lacks substance for electrons with a spherical Fermi surface. However, recent compelling evidence for a d-wave symmetry of the energy gap in high-temperature superconductors has rejuvenated interest in such pairing mechanisms for charge carriers that are coupled solely by a repulsive Coulomb potential.

Scalapino and others[11] computed numerically the spin-fluctuation exchange for two-dimensional tight-binding mod-

els and found very small superconducting transition temperatures for a *d*-state in lowest order. Nevertheless, they pointed out that the random-phase approximation (RPA) series for the susceptibility may boost the pairing strength. In this context, vertex corrections may reduce the RPA enhancement, as pointed out by Schrieffer.[12]

A nested Fermi-surface topology enhances the *d*-wave pairing interaction to yield a *d*-wave superconducting state with $T_c \simeq 100$ K in the leading order spin-fluctuation process, even though the high-T_c regime is constrained to a narrow range of nesting vectors.[13] Higher-order terms are also needed to test this nesting mechanism for enhanced *d*-state superconductivity.

We develop the many-body formalism in Sec. II, including a simple derivation of the scaling and NFL damping. In Sec. III the Ward identity is used to guide the vertex formalism and a perturbation theory calculation verifies that scaling is preserved. The static limit for the susceptibility is computed analytically in Sec. III, and then self-energy and vertex contributions are compared to the standard RPA terms in the context of the SDW phase transition and *d*-wave superconductivity in Sec. IV. Conclusions of our study are in Sec. V.

II. MANY-BODY METHOD

We consider the Hubbard Hamiltonian

$$H=\sum_{\mathbf{k},\sigma} \varepsilon_0(\mathbf{k}) c^+_{\mathbf{k},\sigma} c_{\mathbf{k},\sigma} + \frac{U}{2V} \sum_{\mathbf{k},\mathbf{k}',\mathbf{q},\sigma} c^+_{\mathbf{k}+\mathbf{q},\sigma} c^+_{\mathbf{k}'-\mathbf{q},-\sigma} c_{\mathbf{k}',-\sigma} c_{\mathbf{k},\sigma}, \tag{4}$$

where U defines the on-site Coulomb repulsion, and the electron energy is $\varepsilon_0(\mathbf{k})$.

The noninteracting quasiparticle Green's function is

$$G_0(\mathbf{k},i\omega)=\frac{1}{i\omega-\varepsilon_0(\mathbf{k})}. \tag{5}$$

Dyson's equation

$$G^{-1}(\mathbf{k},i\omega)=G_0^{-1}(\mathbf{k},i\omega)-\Sigma(\mathbf{k},i\omega) \tag{6}$$

defines the self-energy

$$\Sigma(\mathbf{k},i\omega)=-\int \frac{d^dq}{(2\pi)^d} T\sum_{\nu} G(\mathbf{k}+\mathbf{q},i\omega+i\nu) \times D(\mathbf{q},i\nu)\Gamma(\mathbf{k},i\omega;\mathbf{q},i\nu), \tag{7}$$

which is shown diagrammatically in Fig. 1. The screened interaction is defined as

$$D(\mathbf{q},i\nu)=\frac{U}{1+U\Pi(\mathbf{q},i\nu)}, \tag{8}$$

and the polarizability

$$\Pi(\mathbf{q},i\nu)=-2\int \frac{d^dk}{(2\pi)^d} T\sum_{\omega} G(\mathbf{k},i\omega) \times G(\mathbf{k}+\mathbf{q},i\omega+i\nu)\Gamma(\mathbf{k},i\omega;\mathbf{q},i\nu) \tag{9}$$

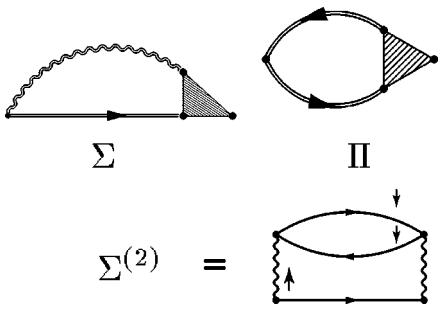

FIG. 1. Diagrams for the Dyson equation for the full self-energy Σ and the dressed susceptibility Π. The shaded triangles represent the vertex, the double wavy line is the screened Coulomb repulsion, and double solid straight lines indicate that the electron Green's function includes the self-energy. The lowest-order Born approximation for the self-energy $\Sigma^{(2)}$ emanates from the Hubbard on-site coupling (wavy line) between electrons of opposite spin.

is also displayed in Fig. 1.

If a noninteracting system exhibits the nesting property in Eq. (3) for some nesting vector $\mathbf{Q}$, then the imaginary part of the bare polarizability[5] develops scaling in ω/T. An elementary proof of this scaling phenomena follows from the polarizability formula in terms of the Fermi function $f(z)=[\exp(z)+1]^{-1}$:

$$\Pi_0''(\mathbf{Q},\omega)=\int \frac{d^dk}{(2\pi)^d}\{f[\varepsilon(\mathbf{k})]-f[\varepsilon(\mathbf{k}+\mathbf{Q})]\} \times \delta[\omega-\varepsilon(\mathbf{k}+\mathbf{Q})+\varepsilon(\mathbf{k})]. \tag{10}$$

Defining a variable $z=\varepsilon(\mathbf{k})=-\varepsilon(\mathbf{k}+\mathbf{Q})$ and then performing the one-dimensional integral over the δ function, one obtains

$$\Pi''_{NFL,0}(\mathbf{Q},\omega)=\frac{\pi}{2}N_0 \tanh\left(\frac{\omega}{4T}\right), \tag{11}$$

which is a function of ω/T only, and is proportional to ω/T for $\omega \ll T$, and then becomes constant for $\omega \gg T$.

By contrast, a conventional electron gas susceptibility is linear in ω (with a negligible temperature dependence), and this analytic structure produces the weak Fermi-liquid damping in Eq. (1).

When electrons scatter between nested orbit regions, the scaling leads to the anomalous damping in the Born approximation. Taking the imaginary part of the self-energy in Eq. (7), and using the leading vertex term $\Gamma=1$, gives

$$\Sigma''_{NFL}(\omega)=-\frac{1}{2}U^2N_0\int d\omega' \left\{\coth\left(\frac{\omega'}{2T}\right)-\tanh\left(\frac{\omega'-\omega}{2T}\right)\right\} \times \Pi''_{NFL,0}(\mathbf{Q},\omega'). \tag{12}$$

Given the scaling of $\Pi''_{NFL,0}(\mathbf{Q},\omega')$ as a function of $y=\omega'/T$, it is readily seen that the quasiparticle damping (in the static $\omega=0$ limit) is proportional to T. At zero temperature, the thermal factors in Eq. (12) reduce to Heaviside functions, and the polarizability saturates to $\Pi''_{NFL}(\mathbf{Q},\omega') \simeq (\pi/2)N_0 \simeq$ const; then the frequency integration gives a simple derivation of $\Sigma''_{NFL}=-\pi\omega[UN_0]^2/2$, which exhibits

the surprising linear frequency variation that is typical of high-temperature superconductors.

III. SELF-ENERGY AND VERTEX CORRECTIONS

A. General formulas and Ward identity

The on-site Hubbard interaction U in Eq. (4), (here U has the dimension energy×unit-cell volume), allows us to decompose the screened interaction, the polarizability, and the vertex according to the subscripts $\parallel$ and $\perp$ that indicate the relative spin orientation of the interacting electrons as parallel and antiparallel respectively. Then we obtain

$$D_{\parallel}(\mathbf{q},i\nu)=\frac{-U^2\Pi_{\parallel}(\mathbf{q},i\nu)}{[1+U\Pi_{\perp}(\mathbf{q},i\nu)]^2-[U\Pi_{\parallel}(\mathbf{q},i\nu)]^2}, \quad (13)$$

$$D_{\perp}(\mathbf{q},i\nu)=\frac{U[1+U\Pi_{\perp}(\mathbf{q},i\nu)]}{[1+U\Pi_{\perp}(\mathbf{q},i\nu)]^2-[U\Pi_{\parallel}(\mathbf{q},i\nu)]^2}, \quad (14)$$

$$\Pi_{\parallel;\perp}(\mathbf{q},i\nu)=-\int \frac{d^dk}{(2\pi)^d}T\sum_{\omega} G(\mathbf{k},i\omega)G(\mathbf{k}+\mathbf{q},i\omega+i\nu) \times\Gamma_{\parallel;\perp}(\mathbf{k},i\omega;\mathbf{q},i\nu), \quad (15)$$

and

$$\Sigma(\mathbf{k},i\omega)=-\int \frac{d^dq}{(2\pi)^d}T\sum_{\nu} G(\mathbf{k}+\mathbf{q},i\omega+i\nu) \times[D_{\parallel}(\mathbf{q},i\nu)\Gamma_{\parallel}(\mathbf{k},i\omega;\mathbf{q},i\nu) +D_{\perp}(\mathbf{q},i\nu)\Gamma_{\perp}(\mathbf{k},i\omega;\mathbf{q},i\nu)]. \quad (16)$$

Charge conservation yields the Ward identity

$$\Gamma_{\parallel}(\mathbf{k},i\omega;\mathbf{q}=0,i\nu)=1-\frac{\Sigma(\mathbf{k},i\omega+i\nu)-\Sigma(\mathbf{k},i\omega)}{i\nu}, \quad (17)$$

and

$$\Gamma_{\perp}(\mathbf{k},i\omega;\mathbf{q}=0,i\nu)=0. \quad (18)$$

In this formulation the charge susceptibility becomes

$$\chi_c(\mathbf{q},i\nu)=2\frac{\Pi_{\parallel}(\mathbf{q},i\nu)+\Pi_{\perp}(\mathbf{q},i\nu)}{1+U[\Pi_{\parallel}(\mathbf{q},i\nu)+\Pi_{\perp}(\mathbf{q},i\nu)]}. \quad (19)$$

and the spin susceptibility is defined as

$$\chi_s(\mathbf{q},i\nu)=2\frac{\Pi_{\parallel}(\mathbf{q},i\nu)-\Pi_{\perp}(\mathbf{q},i\nu)}{1-U[\Pi_{\parallel}(\mathbf{q},i\nu)-\Pi_{\perp}(\mathbf{q},i\nu)]}. \quad (20)$$

If we neglect vertex corrections in the self-energy, we make an error of only second order in the interaction (as opposed to first order in the general scheme): then

$$\Sigma(\mathbf{k},i\omega)=-\int \frac{d^dq}{(2\pi)^d}T\sum_{\nu} G(\mathbf{k}+\mathbf{q},i\omega+i\nu)D_{\parallel}(\mathbf{q},i\nu). \quad (21)$$

This self-energy approximation and the Ward identity suggest the following equations for the vertices (as displayed in Fig. 2):

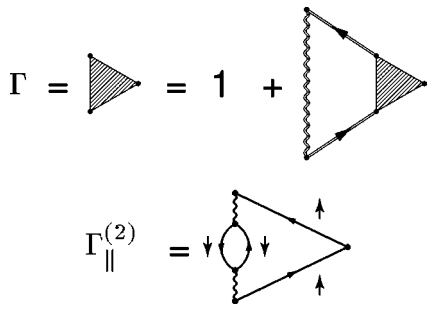

FIG. 2. Graphs for the (shaded) full vertex function Γ, and the leading-order correction that is quadratic in U.

$$\Gamma_{\parallel}(\mathbf{k},i\omega;\mathbf{q},i\nu)=1-\int \frac{d^dk'}{(2\pi)^d}T\sum_{\omega'} D_{\parallel}(\mathbf{k}-\mathbf{k}',i\omega-i\omega') \times G(\mathbf{k}',i\omega')G(\mathbf{k}'+\mathbf{q},i\omega'+i\nu) \times\Gamma_{\parallel}(\mathbf{k}',i\omega';\mathbf{q},i\nu) \quad (22)$$

and

$$\Gamma_{\perp}(\mathbf{k},i\omega;\mathbf{q},i\nu)=0. \quad (23)$$

This last equation implies

$$\Pi_{\perp}(\mathbf{q},i\nu)=0, \quad (24)$$

while

$$\Pi_{\parallel}(\mathbf{q},i\nu)=-\int \frac{d^dk}{(2\pi)^d}T\sum_{\omega} G(\mathbf{k},i\omega) \times G(\mathbf{k}+\mathbf{q},i\omega+i\nu)\Gamma_{\parallel}(\mathbf{k},i\omega;\mathbf{q},i\nu). \quad (25)$$

Equations (23) and (24) appear to be rather restrictive, but will gain support in Sec. III B.

Finally, due to Eq. (24), the screened interactions simplify to

$$D_{\parallel}(\mathbf{q},i\nu)=\frac{-U^2\Pi_{\parallel}(\mathbf{q},i\nu)}{1-[U\Pi_{\parallel}(\mathbf{q},i\nu)]^2} \quad (26)$$

and

$$D_{\perp}(\mathbf{q},i\nu)=\frac{U}{1-[U\Pi_{\parallel}(\mathbf{q},i\nu)]^2}. \quad (27)$$

B. Perturbation theory

In this section we calculate the corrections to the charge and spin susceptibilities to second order in U. The corresponding Feynman diagrams for the polarizability $\Pi_{\parallel}$ are shown in Fig. 3. For $\Pi_{\parallel}$ the simple noninteracting quasiparticle bubble is given by

$$\Pi^{(0)}_{\parallel}(\mathbf{q},i\nu)=-\int \frac{d^dk}{(2\pi)^d}T\sum_{\omega} G_0(\mathbf{k},i\omega)G_0(\mathbf{k}+\mathbf{q},i\omega+i\nu) =-\int \frac{d^dk}{(2\pi)^d}\frac{f[\varepsilon_0(\mathbf{k})]-f[\varepsilon_0(\mathbf{k}+\mathbf{q})]}{i\nu-\varepsilon_0(\mathbf{k}+\mathbf{q})+\varepsilon_0(\mathbf{k})}. \quad (28)$$

The self-energy insertions in Fig. 2 yield

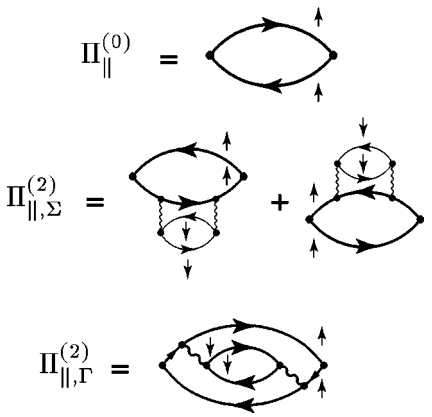

FIG. 3. The noninteracting electron polarizability is a bare bubble, in comparison to polarizabilities that include the self-energy contributions and the vertex correction to second order in U.

$$\Pi_{\parallel}^{(2)}(\mathbf{q},i\nu)_{\Sigma}=-\int \frac{d^dk}{(2\pi)^d}T\sum_{\omega}[G_0(\mathbf{k},i\omega)]^2\Sigma^{(2)}(\mathbf{k},i\omega)\times[G_0(\mathbf{k}+\mathbf{q},i\omega+i\nu)+G_0(\mathbf{k}-\mathbf{q},i\omega-i\nu)], \tag{29}$$

where the leading term in the self-energy is

$$\Sigma^{(2)}(\mathbf{k},i\omega)=U^2\int \frac{d^dk'}{(2\pi)^d}T\sum_{\omega'}\times\Pi_{\parallel}^{(0)}(\mathbf{k}-\mathbf{k}',i\omega-i\omega')G_0(\mathbf{k}',i\omega'). \tag{30}$$

The vertex correction to the polarizability in Fig. 3 is given by

$$\Pi_{\parallel}^{(2)}(\mathbf{q},i\nu)_{\Gamma}=-\int \frac{d^dk}{(2\pi)^d}T\sum_{\omega} G_0(\mathbf{k},i\omega)\times G_0(\mathbf{k}+\mathbf{q},i\omega+i\nu)\Gamma_{\parallel}^{(2)}(\mathbf{k},i\omega;\mathbf{q},i\nu) \tag{31}$$

with the leading correction to the vertex

$$\Gamma_{\parallel}^{(2)}(\mathbf{k},i\omega;\mathbf{q},i\nu)=U^2\int \frac{d^dk'}{(2\pi)^d}T\sum_{\omega'}\Pi_{\parallel}^{(0)}(\mathbf{k}-\mathbf{k}',i\omega-i\omega')\times G_0(\mathbf{k}',i\omega')G_0(\mathbf{k}'+\mathbf{q},i\omega'+i\nu). \tag{32}$$

The expression for $\Pi_{\perp}$ is cumbersome in second order, but its contribution may be finessed by means of the following theorem.

1. Particle-hole symmetry theorem

In the case of a symmetric half-filled energy band, Djajaputra and Ruvalds[14] proved a theorem that shows that diagrams with an odd number of particle lines are canceled exactly by the corresponding graphs that have hole propagators. Charge-conjugation symmetry is the physical origin of this cancelation by analogy to the Furry theorem in quantum electrodynamics. However, band structures of metals limit the applicability of the theorem to a short-range interaction, such as the Hubbard U.

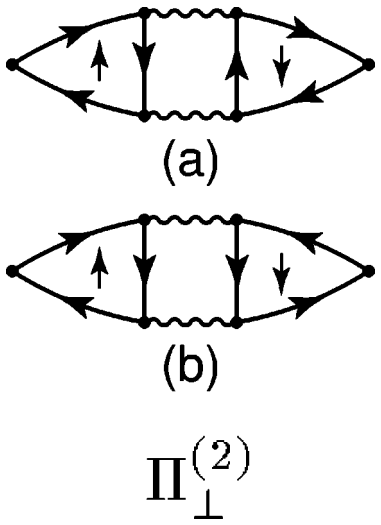

FIG. 4. Diagrams for $\Pi_{\perp}$ that cancel each other exactly when particle-hole symmetry is valid.

This theorem is relevant to nearly half-filled tight-binding models that yield nesting when the chemical potential is close to half filling. For perfect nesting, the Green's function identity $G(-\mathbf{k}+\mathbf{Q},-i\omega)=-G(\mathbf{k},i\omega)$ shows that graphs like the second order $\Pi_{\perp}^{(2)}$ corrections in Fig. 4 cancel each other exactly. Thus we neglect these contributions, even though nesting conditions away from half filling could produce a small correction.

2. Nesting approximation

If the noninteracting electron energy satisfies the nesting property defined in Eq. (3), then

$$\Pi_{\parallel}^{(0)}(\mathbf{Q},i\nu)=\int d\varepsilon N_0(\varepsilon)\frac{\tanh(\varepsilon/2T)}{i\nu+2\varepsilon}, \tag{33}$$

where $N_0(\varepsilon)$ is the density of states. For a symmetric flat density of states $N_0(\varepsilon)=N_0\Theta(W/2-|\varepsilon|)$ the above expression is logarithmically divergent in the static limit:

$$\Pi_{\parallel}^{(0)}(\mathbf{Q},i\nu=0)=N_0\int_{-W/4T}^{W/4T}dx\frac{\tanh(x)}{2x}=N_0\ \ln(\gamma W/\pi T). \tag{34}$$

Here $\gamma=1.781\ldots$ is related to the Euler constant.

Furthermore, the *nesting approximation*[5] suggests the replacement of $\Pi_{\parallel}^{(0)}$ in Eqs. (30) and (32) by its value at the nesting vector $\mathbf{Q}$:

$$\Pi_{\parallel}^{(0)}(\mathbf{k}-\mathbf{k}',i\omega-i\omega')\rightarrow\Pi_{\parallel}^{(0)}(\mathbf{Q},i\omega-i\omega'). \tag{35}$$

When this change is made simultaneously in both the self-energy and vertex, it is a conserving approximation. The self-energy can now be expressed as

$$\Sigma^{(2)}(\mathbf{k},i\omega)=\frac{U^2}{2}\int d\varepsilon' N_0(\varepsilon')\int d\varepsilon'' N_0(\varepsilon'') \times\frac{[\tanh(\varepsilon'/2T)+\coth(\varepsilon''/T)]\tanh(\varepsilon''/2T)}{i\omega-\tilde{\varepsilon}}, \tag{36}$$

which is independent of $\mathbf{k}$, with $\tilde{\varepsilon}=\varepsilon'+2\varepsilon''$.

For the polarization at the nesting vector, we need to evaluate the vertex at $\mathbf{Q}$ as

$$\Gamma_{\parallel}^{(2)}(\mathbf{k},i\omega;\mathbf{Q},i\nu) =\frac{U^2}{2}\int d\varepsilon' N_0(\varepsilon')\int d\varepsilon'' N_0(\varepsilon'') \times\frac{[\tanh(\varepsilon'/2T)+\coth(\varepsilon''/T)]\tanh(\varepsilon''/2T)}{i\nu+2\varepsilon'} \times\left(\frac{1}{i\omega-\tilde{\varepsilon}}-\frac{1}{i\omega+i\nu+\tilde{\varepsilon}}\right), \tag{37}$$

which is also independent of $\mathbf{k}$.

Finally, using the above expressions we obtain the following formulas for the self-energy and vertex corrections to $\Pi_{\parallel}$:

$$\Pi_{\parallel}^{(2)}(\mathbf{Q},i\nu)_{\Sigma}=\frac{U^2}{2}\int d\varepsilon N_0(\varepsilon)\int d\varepsilon' N_0(\varepsilon')\int d\varepsilon'' N_0(\varepsilon')[\tanh(\varepsilon'/2T)+\coth(\varepsilon''/T)]\tanh(\varepsilon''/2T) \times\left\{\frac{\tanh(\varepsilon/2T)}{(i\nu+2\varepsilon)^2}\left[\frac{1}{i\nu+\varepsilon+\tilde{\varepsilon}}-\frac{1}{\varepsilon-\tilde{\varepsilon}}\right]+\frac{1}{(\varepsilon-\tilde{\varepsilon})^2}\left[\frac{\tanh(\tilde{\varepsilon}/2T)}{i\nu+\varepsilon+\tilde{\varepsilon}}-\frac{\tanh(\varepsilon/2T)}{i\nu+2\varepsilon}\right]+\frac{\cosh^{-2}(\varepsilon/2T)/2T}{(i\nu+2\varepsilon)(\varepsilon-\tilde{\varepsilon})}\right\}, \tag{38}$$

and

$$\Pi_{\parallel}^{(2)}(\mathbf{Q},i\nu)_{\Gamma}=-\frac{U^2}{2}\int d\varepsilon N_0(\varepsilon)\int d\varepsilon' N_0(\varepsilon')\int d\varepsilon'' N_0(\varepsilon'')\,\frac{[\tanh(\varepsilon'/2T)+\coth(\varepsilon''/T)]\tanh(\varepsilon''/2T)}{(i\nu+2\varepsilon)(i\nu+2\varepsilon')} \times\left[\frac{\tanh(\varepsilon/2T)-\tanh(\tilde{\varepsilon}/2T)}{\tilde{\varepsilon}-\varepsilon}+\frac{\tanh(\varepsilon/2T)+\tanh(\tilde{\varepsilon}/2T)}{i\nu+\varepsilon+\tilde{\varepsilon}}\right]. \tag{39}$$

3. Scaling conservation

The key ingredient of scaling refers to the property that the noninteracting electron susceptibility is a function only of ω/T in case of nesting. The proof that this behavior is sustained by self-energy and vertex corrections is obvious from Eqs. (38) and (39). Transforming the threefold integration to dimensionless variables $y=\varepsilon/T$, etc., one sees that the imaginary part of the resulting polarizabilities are simply functions of ω/T by analytic continuation.

This result assures that the vertex corrections as well as the self-energy terms yield the qualitative scaling of the susceptibility that generates the linear T variation of the damping in the NFL theory. Quantitative corrections, and possible effects for the frequency variation of the damping require evaluation of the above integrals, which is unfortunately not feasible analytically in the general case of finite frequency.

4. Static limit

Since according to Eq. (34) the static polarizability at the nesting vector diverges logarithmically, we focus on corrections for $i\nu=0$. Taking this limit in Eqs. (38) and (39) we obtain

$$\Pi_{\parallel}^{(2)}(\mathbf{Q},i\nu=0)_{\Sigma} =\frac{U^2}{2}N_0^3\int_{-x_0}^{x_0}dx\int_{-x_0}^{x_0}dx'\int_{-x_0}^{x_0}dx''[\tanh(x')+\coth(2x'')]\tanh(x'') \times\left\{\frac{1}{(x-\tilde{x})^2}\left[\frac{\tanh(\tilde{x})}{x+\tilde{x}}-\frac{\tanh(x)}{2x}\right]+\frac{\cosh^{-2}(x)}{2x(x-\tilde{x})}\right\} \tag{40}$$

and

$$\Pi_{\parallel}^{(2)}(\mathbf{Q},i\nu=0)_{\Gamma}=-\frac{U^2}{4}N_0^3\int_{-x_0}^{x_0}dx\int_{-x_0}^{x_0}dx'\int_{-x_0}^{x_0} \times dx''[\tanh(x')+\coth(2x'')] \times\tanh(x'')\,\frac{\tanh(x)+\tanh(\tilde{x})}{xx'(x+\tilde{x})}, \tag{41}$$

where we introduced $\tilde{x}=x'+2x''$ and $x_0=W/4T$.

Equations (40) and (41) are logarithmically divergent for large x_0. The leading logarithmic terms can be evaluated as

$$\Pi_{\parallel}^{(2)}(\mathbf{Q},i\nu=0)_{\Sigma}=-N_0\overline{U}^2\left[\frac{1}{2}\ln^2(\gamma W/\pi T)+O(\ln)\right], \tag{42}$$

and

$$\Pi_{\parallel}^{(2)}(\mathbf{Q},i\nu=0)_{\Gamma}=-N_0\overline{U}^2\left[\frac{1}{3}\ln^3(\gamma W/\pi T)+O(\ln^2)\right], \tag{43}$$

where $\overline{U}=N_0U$ is the dimensionless on-site interaction.

We now summarize our results for the polarizabilities at the nesting vector in the static limit. Up to second order in U, the leading logarithmically divergent terms from self-energy and vertex corrections give

$$\begin{aligned}\Pi_{\parallel}(\mathbf{Q},i\nu=0)&=\Pi_{\parallel}^{(0)}(\mathbf{Q},i\nu=0)+\Pi_{\parallel}^{(2)}(\mathbf{Q},i\nu=0)_{\Sigma}\\&\quad+\Pi_{\parallel}^{(2)}(\mathbf{Q},i\nu=0)_{\Gamma}\\&=N_0\ln(\gamma W/\pi T)\left\{1-\overline{U}^2\left[\frac{1}{3}\ln^2(\gamma W/\pi T)\right.\right.\\&\quad\left.\left.+O(\ln)\right]\right\}\end{aligned} \tag{44}$$

and

$$\Pi_{\perp}(\mathbf{Q},i\nu=0)_{\Sigma+\Gamma}=0. \tag{45}$$

IV. CORRESPONDENCE TO RPA

A. Spin susceptibility

The random-phase approximation (RPA) is a standard method in many-body physics. It picks out a geometric series of polarizability bubbles that can be easily summed to yield the spin susceptibility

$$\chi_{S,RPA}\equiv\frac{2\chi_0}{1-U\chi_0}. \tag{46}$$

where $\chi_0=\Pi_{\parallel}^{(0)}$ is the bare polarizability defined in Eq. (33). Obviously the RPA preserves the scaling feature of the susceptibility in the case of nesting. A common application of the RPA is to estimate the transition temperature for a SDW phase transition, which occurs when the denominator in Eq. (46) vanishes; i.e.,

$$U\chi_0'(\mathbf{Q},\omega=0,T_{SDW})=1. \tag{47}$$

Since our analytic results for the self-energy and vertex corrections are valid to second order in U, we compare them to the similar leading terms in the RPA series, which are shown in Fig. 5 and have the static limit

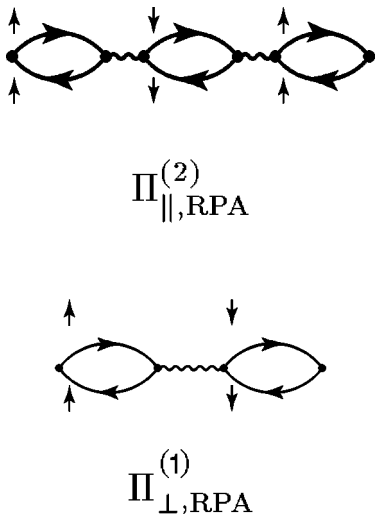

FIG. 5. Leading-order terms for the polarizabilities $\Pi_{\parallel}$ and $\Pi_{\perp}$ in the random-phase approximation.

$$\chi_{S,RPA}^{(2)}(\mathbf{Q},i\nu=0)=2N_0\ln(\gamma W/\pi T)\{1+\overline{U}\ln(\gamma W/\pi T)+\overline{U}^2\ln^2(\gamma W/\pi T)\}. \tag{48}$$

By contrast to the RPA enhancement, both principal self-energy (Σ) and vertex (Γ) corrections in Eqs. (42) and (43) reduce the susceptibility. Their combined influence in leading logarithmic approximation can be expressed as

$$\Delta\chi_{S,\Sigma+\Gamma}(\mathbf{Q},i\nu=0)=-\frac{2}{3}\overline{U}^2N_0\ln^3(\gamma W/\pi T). \tag{49}$$

A comparison of these contributions in Fig. 6 reveals that the self-energy and vertex terms substantially reduce the RPA enhancement of the spin susceptibility, although the net

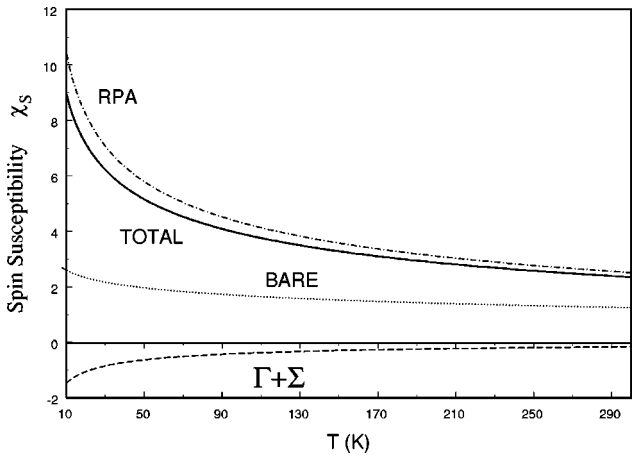

FIG. 6. Comparison of spin-susceptibility corrections as a function of temperature. The noninteracting $2\chi_0$ (dotted curve) diverges logarithmically as a result of nesting. The standard RPA dot-dash curve (to order U^2) overestimates the susceptibility enhancement. Self-energy and vertex corrections $\Delta\chi$ (dashed curve) reduce the susceptibility. The net result of these contributions is the total susceptibility (solid curve) that exceeds the bare $2\chi_0$ by a significant amount when a Coulomb coupling $U=W=1$ eV and a density of states $N_0=0.2\ \mathrm{eV}^{-1}$ are used in these calculations.

result of their combined influence is still an increased susceptibility. The curves in Fig. 6 indicate that the RPA overestimate of the spin susceptibility tends to exaggerate the SDW phase-transition temperature by a significant amount for this choice of a Coulomb repulsion $U \simeq W = 1$ eV. It should be noted that N_0 refers to the the density-of-states portion originating from a nested region, and is chosen as $N_0 = 0.2\ \mathrm{eV}^{-1}$ in the present analysis. Physically one may view nested parallel sides of a nearly square Fermi surface as a source of a modest density-of-states value, while the corners dominate N_0 by virtue of a small quasiparticle group velocity. Hence a realistic model may have rounded corners that yield the main part of the total N_0 whereas nested regions determine the remainder.

These results imply that theories of *d*-wave superconductivity cannot rely solely on the RPA to elevate the coupling parameter. Nevertheless, there remains a limited net increase in the susceptibility from the combined RPA+self-energy +vertex terms (by less than a factor of 2), and this positive influence reduces the need for large-U values to fit experimental conductivity data on high-temperature superconductors. However, acceptable U values cannot dip to the weak-coupling regime $U \ll W$, where these many-body corrections become negligible. Further studies of the susceptibility enhancement at finite frequency are warranted by the present indications in the static limit.

Our analytic results are relevant to the general theory of many-body systems that seeks to identify key diagrams that properly describe physical properties. DuBois[15] originally noted that the self-energy of an electron gas can offset the vertex influence, but the mathematical complexity of the momentum and frequency variation of the Coulomb potential vertex has thwarted a full rigorous solution. Nevertheless, progress has been achieved for special cases, with reasonable simplifying approximations. Rajagopal[16] solved the integral equation for a vertex function originating from a Yukawa potential by means of a variational approach. Many groups have applied physical insight and sum rule constraints to derive local-field corrections to the susceptibility.[1] Engel and Vosko[17] obtained self-energy and vertex corrections for the Coulomb gas at zero temperature, and reduced the results to one-dimensional integrals in the special limit $\omega = 0$.

The case of the Hubbard model has also been analyzed by many groups. A particular conserving approximation (named FLEX) was developed by Bickers and Scalapino,[18] which emphasizes the Parquet ladder series of graphs. Their numerical computations[19] on a tight-binding lattice model reveal a net increase in the susceptibility that is qualitatively in accord with our analytic results—even though their Fermi surface is not nested. Their Monte Carlo simulations also provide a convenient target susceptibility for comparison in the large temperature regime. Another numerical study of the second order self-energy and vertex corrections for a tight-binding model by Hotta and Fujimoto[20] shows the trend of a susceptibility reduction by self-energy and vertex corrections. Tremblay's group also found a susceptibility in Monte Carlo simulations[21] that implies that the vertex and self-energy terms (to all orders in U) partially cancel the RPA graphs.

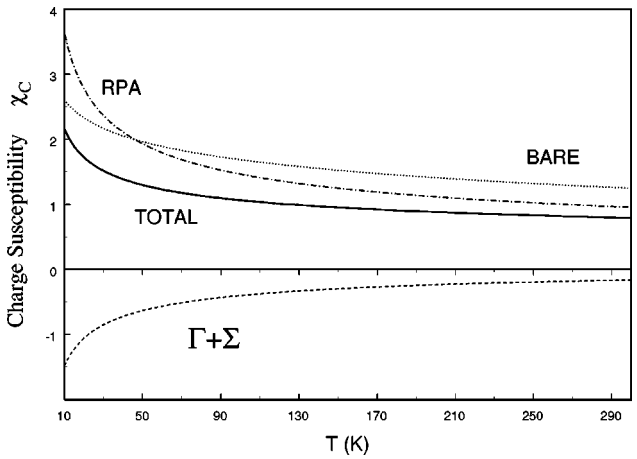

FIG. 7. Suppression of the charge susceptibility by self-energy and vertex corrections (dashed curve) overwhelms the RPA series (dot-dash curve) and leads to a total susceptibility (solid curve) that is below the noninteracting case shown by the dotted curve. A Coulomb coupling $U = W = 1$ eV and a density of states $N_0 = 0.2\ \mathrm{eV}^{-1}$ are used in these calculations.

B. Charge susceptibility

A striking suppression of the charge susceptibility by strong Coulomb correlations occurs because the leading RPA term has opposite sign, as seen below:

$$\chi^{(2)}_{C,RPA}(\mathbf{Q}, i\nu = 0) = 2N_0 \ln(\gamma W/\pi T) \times \{1 - \overline{U} \ln(\gamma W/\pi T) + \overline{U}^2 \ln^2(\gamma W/\pi T)\}. \tag{50}$$

On the other hand, the relevant self-energy and vertex corrections are both negative, and the leading logarithmic term of Eq. (49) also serves to yield the total charge susceptibility

$$\chi^{(2)}_{C,Total}(\mathbf{Q}, i\nu = 0) = 2N_0 \ln(\gamma W/\pi T) \times \left\{ 1 - \overline{U} \ln(\gamma W/\pi T) + \frac{2}{3} \overline{U}^2 \ln^2(\gamma W/\pi T) \right\}. \tag{51}$$

Thus the total charge susceptibility is severely diminished by the combination of these correlations, as illustrated by the solid curve in Fig. 7 with $U = W = 1$ eV and $N_0 = 0.2\ \mathrm{eV}^{-1}$. This type of reduction for the charge susceptibility has been noted previously by others[20,21] in numerical computations of tight-binding models without nesting.

The above reduction in the charge susceptibility stems primarily from the vertex correction (shown by the dashed curve in Fig. 7), and may explain why some organic metals and high-temperature superconductors are not inclined to form charge-density waves[22] (CDW). Balseiro and Falicov[23] proved that a nested Fermi surface favors a CDW phase transition over a standard BCS superconducting state for a fixed value of the electron-phonon coupling λ, and many organic metals with partial nesting indeed exhibit CDW states at high temperatures.

But other organic metals—and superconducting cuprates—transform to antiferromagnetic materials when their chemical composition is changed slightly. Traditionally such tendencies toward SDW order indicate that the Coulomb U dominates the electron-phonon coupling λ in these materials. Moreover, the present results demonstrate that strong electron correlations deplete the charge susceptibility and thus reduce the likelihood of CDW formation even when a normal value of λ occurs.

For a given intermediate strength $U=W$, the renormalized charge susceptibility in Fig. 7 is much weaker than the spin susceptibility in Fig. 6. Within the Hubbard model, it therefore appears that the exchange of charge fluctuations will be less important than the pairing induced by spin fluctuations in theories of d-wave superconductivity.

V. CONCLUSIONS

The basic scaling, which originates from a nested Fermi surface, is maintained when self-energy, vertex, and RPA corrections are calculated in leading orders of perturbation theory. Although self-energy and vertex contributions counteract the standard RPA series enhancement of the spin susceptibility, the total renormalized spin susceptibility remains considerably larger than the noninteracting case.

If the renormalized susceptibility is used to compute the anomalous damping that is a key property of high-temperature superconductors, the prerequisite scaling form of the enhanced susceptibility allows the NFL theory to fit conductivity experiments on cuprates with values of the Coulomb repulsion U that are smaller than the original Born approximation estimates of $U=W$. Hence the magnitude of the quasiparticle scattering cross section suggests an intermediate strength of U that is less than the bandwidth.

Conventional treatments of spin-density-wave phase transitions by the RPA approximation may be improved by including self-energy and vertex corrections. In the static limit, our analytic expressions for the polarizability (with self-energy and vertex corrections in leading order) reveal that the standard RPA approach overestimates the SDW phase transition temperature for a nested Fermi surface. At low temperatures the self-energy and vertex corrections diverge logarithmically, in line with similar divergences in the bare susceptibility and the RPA terms. Thus the validity of the present perturbation analysis breaks down at low T. Within RPA the SDW phase-transition temperature sets an approximate lower limit, although the vertex correction reduces this barrier somewhat.

In realistic situations the nesting approximation breaks down at some temperature T^* that marks the crossover to ordinary Fermi-liquid behavior below T^*. Hence, for $T<T^*$ there will not be any logarithmic singularities in the self-energy, vertex, or polarizability. This physical boundary represents actual materials that have Fermi surfaces and finite effective-mass enhancements, even though they exhibit CDW or SDW phase transitions at reasonably high temperatures. In the case of high-temperature superconductors, the crossover temperature T^* can be varied by adjusting the oxygen content or distorting the Fermi surface by other means; thus a crossover from the anomalous (linear T) damping to a standard T^2 Fermi-liquid variation is often seen. It is interesting to note that high superconducting transition temperatures are found only in those cuprate alloys where the chemical composition suits the condition for anomalous damping.

Considering the recent widespread evidence for d-wave superconductivity in cuprates, the prospect of pairing electrons (or holes) by a spin-fluctuation exchange method requires reliable information for the susceptibility. Although the self-energy and vertex parts produce a detrimental pairing impact, as implied by our results for the spin susceptibility, the RPA terms exceed the combined Σ and Γ contributions: Hence a limited net increase (up to a factor of 2) may be plausible for the momentum average of the spin susceptibility that determines the d-wave pairing. However, claims for a much larger pairing enhancement by higher-order RPA terms (whose sum diverges near a SDW instability) are not trustworthy without examination of competing higher-order self-energy and vertex corrections.

A revival of interest in the possibility of room-temperature superconductivity in metallic hydrogen[24] has stimulated new studies of the effective interactions between two electrons in a Coulomb gas. Kukkonen and Overhauser[25] used a self-consistent perturbation theory to derive an effective electron-electron coupling that includes exchange and correlation effects. Vignale and Singwi[26] employed diagrammatic techniques to derive a similar potential, with nonlocal additions, and Richardson and Ashcroft[24] have extended these results to include self-energy contributions. Together with our present results for a nesting approximation, these theories should provide guidance for future computations of superconducting pairing in metals with nested Fermi surfaces.

Charge-fluctuation effects are diminished notably by the vertex and self-energy terms that counteract the leading RPA contributions to the charge susceptibility. We find that the total charge susceptibility is significantly smaller than the bare susceptibility, to second order in U, when the Coulomb repulsion is comparable to the bandwidth. Hence these electron correlations diminish the chances for creating charge-density waves in nesting situations where the electron-phonon coupling would otherwise enable a CDW instability to compete with classic BCS superconductivity.

Furthermore, since the renormalized spin susceptibility is much larger than the charge susceptibility—as a consequence of these second-order interactions—it appears that spin fluctuations should dominate the quasiparticle collision cross section. By the same token, spin fluctuations should be favored as a mechanism for d-wave pairing interactions in a Hubbard model with nesting.

Our analytic results are compatible with research on vertex corrections for alternate nesting models. Numerical computations for a square Fermi surface yield vertex corrections as a function of momentum as well as frequency[27] and the magnitude of the vertex at the nesting vector is similar to the present analytic expression. Another nesting model, i.e., an approximate square with rounded corners, has been investigated by the Parquet diagram method, which clarifies the competition between d-wave superconductivity and the SDW.[28] Sum rules and conservation principles for various theoretical techniques (including the RPA) have recently been surveyed by Tremblay's group.[21]

ACKNOWLEDGMENTS

We thank D. Djajaputra for many stimulating comments and technical assistance. We appreciate discussions with C. T. Rieck, S. Tewari, and A. Zawadowski. This research was supported by the U.S. Department of Energy Grant No. DEFG05-84ER45113 and a stipend from the Center of Advanced Studies at the University of Virginia. A.V. is supported by HNRF Grants No. OTKA T016740 and No. T020030.

[1] G. D. Mahan, *Many-Particle Physics* (Plenum, New York, 1990).
[2] J. M. Luttinger, Phys. Rev. **121**, 942 (1961).
[3] J. Ruvalds, Supercond. Sci. Technol. **9**, 905 (1996).
[4] C. M. Varma, P. B. Littlewood, S. Schmitt-Rink, E. Abrahams, and A. E. Ruckenstein, Phys. Rev. Lett. **63**, 1996 (1989).
[5] A. Virosztek and J. Ruvalds, Phys. Rev. B **42**, 4064 (1990).
[6] J. Ruvalds and A. Virosztek, Phys. Rev. B **43**, 5498 (1991).
[7] A. Virosztek and J. Ruvalds, Phys. Rev. Lett. **67**, 1657 (1991).
[8] A. W. Overhauser, Phys. Rev. **128**, 1437 (1962).
[9] N. F. Berk and J. R. Schrieffer, Phys. Rev. Lett. **17**, 433 (1966).
[10] W. Kohn and J. M. Luttinger, Phys. Rev. Lett. **15**, 524 (1965).
[11] D. J. Scalapino, Phys. Rep. **250**, 329 (1995).
[12] J. R. Schrieffer, J. Low Temp. Phys. **99**, 397 (1995).
[13] J. Ruvalds, C. T. Rieck, S. Tewari, J. Thoma, and A. Virosztek, Phys. Rev. B **51**, 3797 (1995).
[14] D. Djajaputra and J. Ruvalds, Solid State Commun. (to be published).
[15] D. F. DuBois, Ann. Phys. (N.Y.) **7**, 174 (1959); **8**, 24 (1959).
[16] A. K. Rajagopal, Phys. Rev. A **6**, 1239 (1972).
[17] E. Engel and S. H. Vosko, Phys. Rev. B **42**, 4940 (1990).
[18] N. E. Bickers and D. J. Scalapino, Ann. Phys. (N.Y.) **193**, 206 (1989).
[19] N. E. Bickers, D. J. Scalapino, and S. R. White, Phys. Rev. Lett. **62**, 961 (1989).
[20] T. Hotta and S. Fujimoto, Phys. Rev. B **54**, 5381 (1996).
[21] Y. M. Vilk and A.-M. S. Tremblay, J. Phys. I **7**, 1309 (1997).
[22] G. Gruner, *Density Waves in Solids* (Addison-Wesley, Reading, MA, 1994).
[23] C. A. Balseiro and L. M. Falicov, Phys. Rev. B **20**, 4457 (1979).
[24] C. F. Richardson and N. W. Ashcroft, Phys. Rev. Lett. **78**, 118 (1997).
[25] C. A. Kukkonen and A. W. Overhauser, Phys. Rev. B **20**, 550 (1979).
[26] G. Vignale and K. S. Singwi, Phys. Rev. B **32**, 2156 (1985).
[27] D. Djajaputra and J. Ruvalds, cond-mat/9712052 (unpublished).
[28] A. T. Zheleznyak, V. M. Yakovenko, and I. E. Dzyaloshinskii, Phys. Rev. B **55**, 3200 (1997).